Available online at www.sciencedirect.com
SCIENCE DIRECT®
Bioorganic & Medicinal Chemistry
Bioorganic & Medicinal Chemistry 13 (2005) 6035–6044

Antitumor activity and distribution of pyrroloiminoquinones in the sponge genus *Zyzzya*

Marie-Geneviève Dijoux,[a,†] Peter C. Schnabel,[b,‡] Yali F. Hallock,[a,§] Jamie L. Boswell,[a,¶,**] Tanya R. Johnson,[a,††] Jennifer A. Wilson,[a,††] Chris M. Ireland,[c] Rob van Soest,[d] Michael R. Boyd,[a,‡‡] Louis R. Barrows[b,*] and John H. Cardellina, II[a,*,¶]

[a]*Laboratory of Drug Discovery Research and Development, Developmental Therapeutics Program, Division of Cancer Treatment and Diagnosis, National Cancer Institute-Frederick Cancer Research & Development Center, Building 1052-Room 121, Frederick, MD 21702-1201, USA*
[b]*Department of Pharmacology and Toxicology, College of Pharmacy, University of Utah, Salt Lake City, UT 84112, USA*
[c]*Department of Medicinal Chemistry, College of Pharmacy, University of Utah, 308 Skaggs Hall, Salt Lake City, UT 84112, USA*
[d]*Zoölogisch Museum of the University of Amsterdam, Mauritskade 61, PO Box 94766, 1090 GT Amsterdam, The Netherlands*

Received 5 April 2005; revised 7 June 2005; accepted 7 June 2005
Available online 11 July 2005

Abstract—A detailed analysis of four different collections of the sponge genus *Zyzzya* yielded nine pyrroloiminoquinones of the makaluvamine, batzelline, and isobatzelline/damirone classes. Dereplication analyses of additional *Zyzzya* extracts did not disclose more potent or additional new compounds. Comparative testing of these compounds in the National Cancer Institute's 60 cell line human tumor screen revealed varying levels of potency and differential cytotoxicity, apparently related to the unsaturation levels in and substitution patterns on the core ring system. Further studies on the topoisomerase II-mediated DNA cleavage were conducted. Reductive activation of the pyrroloiminoquinones led to DNA damage in vitro, which correlated with half wave potentials and reversibility parameters. DNA damage could be abrogated by ascorbate. Fluorescence displacement was used to measure intercalation with DNA; intercalation efficiency did not correlate with DNA-damaging proficiency. Makaluvamine H (**5**) emerged as the most potent and differential of our isolates, roughly comparable to makaluvamines C (in vitro) and I (in vivo). 3,7-Dimethyl guanine was isolated from one of the *Zyzzya* collections and from the sponge *Latrunculia purpurea*.

Keywords: Antitumor; Pyrroloiminoquinone; Topoisomerase II; DNA intercalation; DNA damage; *Zyzzya*.

* Corresponding authors. Tel.: +1 801 581 6287; fax: +1 801 585 5111 (L.R.B.); tel.: +1 301 846 1121; fax: +1 301846 6775 (J.H.C.); e-mail addresses: lbarrows@deans.pharm.utah.edu; jcardellina@ncifcrf.gov
† Recipient of a postdoctoral fellowship from the Conseil Régional de Champagne-Ardenne (France); Present address: Laboratoire de Pharmacognosie, DPM UMR 5063 CNRS-Université Joseph Fourier, France.
‡ Present address: Saba University School of Medicine, P.O. Box 1000, The Bottom, Saba, Netherlands-Antilles.
§ Present address: Grants & Contracts Operations Branch, DTP, DCTD, NCI, 6130 Executive Boulevard, Suite 8058, Rockville, MD 20852, USA.
¶ Present address: Screening Technologies Branch, DTP, DCTD, NCI, Bldg 440, Frederick, MD 21702-1201, USA.
** Werner H. Kirsten Student Intern, 1996–1997; Undergraduate Student Research Trainee, 1997–1998.
†† Present address: Molecular Targets Development Program, CCR, NCI, Bldg 1052, Frederick, MD 21702-1201, USA.
‡‡ Present address: USA Cancer Research Institute, University of Southern Alabama, Mobile, AL 36608-0002, USA.

0968-0896/$ - see front matter © 2005 Elsevier Ltd. All rights reserved.
doi:10.1016/j.bmc.2005.06.019

1. Introduction

Following the first report of pyrroloiminoquinone alkaloids from sponge extracts,[1] there was rapid growth of interest and effort in this class of distinctively colored compounds. Numerous tricyclic and pentacyclic analogs have been isolated and identified. While sponges have provided the majority of such alkaloids isolated to date, tunicates were subsequently found to contain them as well.[2] Molinski provided an early review on this class of compound,[3] and Faulkner's annual reviews[4] (and now Blunt et al.[5]) have updated progress since then. Antunes et al. have just published a review of the chemistry and bioactivity of this class.[6] Ding et al. have also reviewed these compounds from a pharmacological perspective.[7]

In the course of our continuing search for new antitumor agents from natural sources, we found that numerous extracts from the sponge genus *Zyzzya*[8,9] exhibited very similar and striking differential cytotoxicity profiles

in the National Cancer Institute's (NCI) 60 cell line primary screen.[10] We report here the bioassay-guided isolation, identification, and biological testing of 10 compounds (**1**, **2**, **4**–**10**, **12**) from these extracts, along with the results of comparative testing of makaluvamines C (**16**) and H (**5**) and mechanistic studies.

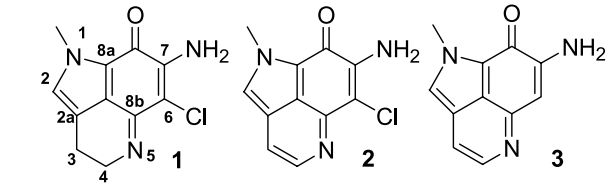

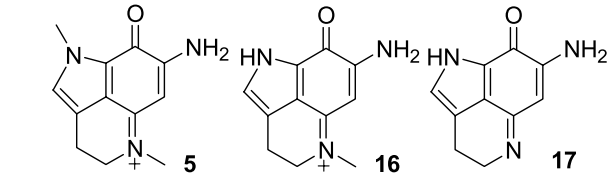

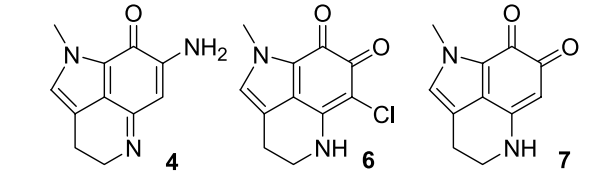

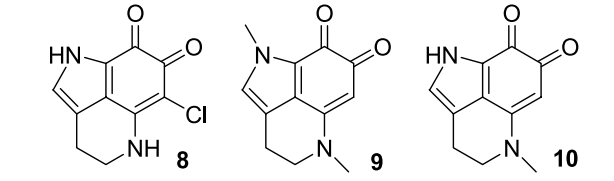

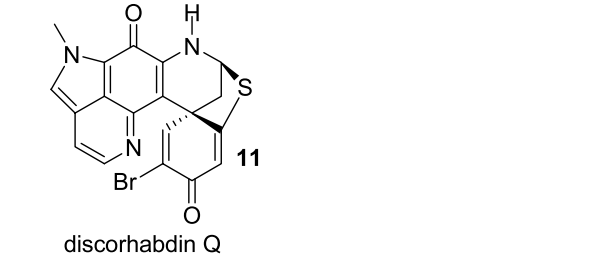

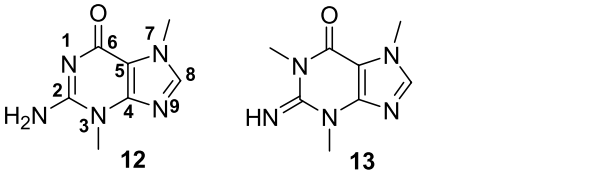

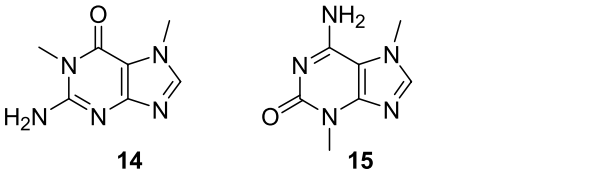

2. Results and discussion

2.1. Chemistry

Specimens of *Zyzzya* from four different sites in Australia revealed somewhat different chemistry, although the aqueous and organic extracts of all the collections (Table 1) were quite cytotoxic. The organic extracts of *Zyzzya fuliginosa* (South Murion Island) yielded the known isobatzelline C[11] (**1**) as a major constituent (10.3% of the extract) upon solvent–solvent partitioning and gel permeation of the active partition fraction through Sephadex LH-20. Comparison of spectral data from our sample with the literature report[11] confirmed the structure.

A collection from Marchinbar Island provided four pyrroloiminoquinones: isobatzelline C (**1**),[11] isobatzelline E (**2**),[12] batzelline C (**6**),[13] and 6-dechlorobatzelline C (**7**). The organic extract was found to contain **1** and **2**, which were separated and purified by solvent–solvent partitioning, followed by Sephadex LH-20 and silica gel vacuum liquid chromatography (VLC).[14] Two approaches were used to separate the aqueous extract. Application of the EtOH precipitation protocol that we employ in the dereplication of anionic polysaccharides and removal of other high molecular weight compounds[15] gave a cytotoxic supernatant fraction from which **1** could be isolated in high yield (~13%) by gel permeation through Sephadex LH-20. Alternatively, partitioning the aqueous extract between *n*-BuOH and H_2O dispersed the cytotoxicity in both fractions. Isobatzelline C (**1**) and 6-dechlorobatzelline C (**7**) were recovered from the H_2O fraction, while **1** and batzelline C (**6**) were isolated from the *n*-BuOH solubles. As was the case for the South Murion Island collection, isobatzelline C was the major cytotoxin in this collection of *Zyzzya massalis*, comprising 37% of the organic extract and >13.5% of the aqueous extract.

The molecular formula of **7** was determined to be $C_{11}H_{10}N_2O_2$ by HRFABMS. The *o*-quinone structure was apparent from the molecular formula, and the absence of chlorine pointed to a damirone analog. The ethano bridge (C_3–C_4) and two aromatic protons were obvious from the ^1H NMR spectrum. Placement of the methyl group at N-1 was suggested by the ^1H and ^{13}C NMR (Table 2) chemical shifts and confirmed by an NOE with H-2. Thus, **7** is identical to the compound obtained by catalytic hydrogenation of batzelline A;[13] this compound has also been reported in a patent,[16] but not as a natural product.

The Goss passage collection of *Z. fuliginosa* yielded only small quantities (~1.2%) of makaluvamine A (**4**) and a trace of batzelline D (**8**),[12] along with small quantities of the guanine derivative **12** from the aqueous extract. Makaluvamine A was readily identified by comparison with literature data.[17]

HRFABMS of **12** provided the molecular formula $C_7H_{10}N_5O$ for the pseudomolecular ion. The ^1H NMR spectrum was quite simple, with a one proton aromatic

Table 1. Extraction/bioassay data for sponge collections

	Organic extract			Aqueous extract			Compounds isolated
	Mass (g)	% dry wt	Mean panel TGI[e] (μg/mL)	Mass (g)	% dry wt	Mean panel GI_{50}[f] (μg/mL)	
Zyzzya fuliginosa[a]	9.13	4.1	0.53	63.80	28.3	ND[g]	**1**
Zyzzya fuliginosa[b]	8.72	5.6	3.1	65.78	42	3.8	**1**, **2**, **6**, **7**
Zyzzya fuliginosa[c]	5.51	5.5	0.11	21.09	21.6	0.1	**4**, **8**, **12**
Zyzzya sp.[d]	4.95	2.3	1.48	27.17	13	10	**5**, **9**, **10**, **11**

[a] From South Murion Island.
[b] From Marchinbar Island.
[c] From Goss passage.
[d] From Assail Bank.
[e] Total growth inhibition (net).
[f] Growth inhibition to 50% controls.
[g] Not determined.

Table 2. 125 MHz ^{13}C NMR data for compounds **1**, **2**, **4–10**

Carbon	**1**[a]	**2**[b]	**4**[a]	**5**[c]	**6**[c]	**7**[a]	**8**[a]	**9**[c]	**10**[c]
1(NMe)	35.9	37.7	35.9	36.6	35.9	39.5		36.0	
2	131.3	130.8	131.1	131.8	129.9	128.8	124.9	127.5	125.2
2a	118.5	124.1	117.8	119.1	117.1	116.5	117.5	115.8	118.5
3	18.0	113.3	18.0	20.3	19.2	19.0	19.1	20.2	21.0
4	43.4	141.5	42.0	54.1	42.0	41.1	41.9	51.9	53.3
5(NMe)				39.8				38.5	38.6
5a	152.5	145.7	156.8	158.1	149.3	153.8	149.4	154.7	157.5
6	92.7	106.5	86.5	86.8	97.3	92.5	97.2	93.4	93.2
7	151.7	144.1	156.1	157.9	169.5	171.6	168.7	171.3	172.4
8	166.0	165.5	168.3	169.0	171.8	177.7	171.8	178.5	180.6
8a	122.5	119.0	123.1	124.8	123.9	124.4	124.3	124.6	125.9
8b	121.4	118.6	122.4	124.4	123.3	123.9	123.1	124.5	126.0

[a] Recorded in DMSO-d_6.
[b] Recorded in $CDCl_3/CD_3OD$ (1:1).
[c] Recorded in CD_3OD.

singlet (δ 7.79), two *N*-methyl groups at δ 3.62 and 3.97, and a broad, exchangeable, three proton singlet at δ 6.87 (in DMSO-d_6). The ^{13}C NMR spectrum contained five aromatic carbons, of which only one was protonated, along with two methyl groups (δ 31.4 and 33.8). These data, the UV spectrum, and EIMS fragmentation pattern pointed to a guanine derivative. NOE experiments revealed the effects between one *N*-methyl and the aromatic proton, and between the other *N*-methyl and the exchangeable protons. HMBC experiments showed correlations of the aromatic proton to C-4 (δ 150.0), C-5 (δ 112.4), and the *N*-methyl (C-11, δ 33.8); the C-11 methyl group was coupled to C-5 and C-8 (δ 142.6). The other *N*-methyl group had correlations to C-4 and C-2 (δ 156.0), while the exchangeable (NH_3^+) protons were correlated with C-2, C-4, and C-6 (δ 164.9). These data led to structure **12**, 3,7-dimethylguanine, which had been reported from a *Latrunculia* sp.[18] Shortly thereafter, we also found quantities of **12** in extracts of *Latrunculia purpurea* from Horseshoe Reef, Australia. The closely related 1,3,7-trimethylguanine (**13**),[19] 1,7,-dimethylguanine (**14**),[20], and 3,7-dimethylisoguanine (**15**)[21] have been reported from the sponges *Latrunculia brevis*, *Jaspis* sp., and *Agelas longissima*, respectively.

A collection of *Zyzzya* sp. from the Assail Bank yielded four compounds from the organic extract. Makaluvamine H[22] [*N*(5)-methyl makaluvamine A, **5**] was the most abundant metabolite (16% of the extract), while damirones A (**9**) and B (**10**)[23] and the new compound discorhabdin Q (16,17-dehydrodiscorhabdin B, **11**)[24] were obtained in much smaller quantities (0.3–1.7%).

2.2. Antitumor activity

Comparative in vitro antitumor screening[10,25] of this group of compounds in the NCI 60 cell line panel provided some intriguing observations. At 50 μg/mL, 3,7-dimethylguanine (**12**) was not cytotoxic to any of the tumor cell lines in the NCI panel. The fully aromatized **2** was only weakly cytotoxic, while isobatzelline C (**1**) displayed relatively potent and differential cytotoxicity (mean panel GI_{50} approximately 10^{-6} M). Barrows et al. have reported similar differences in cytotoxicity for an analogous pair, makaluvamines A and B (**4** and **3**).[26] Makaluvamine H (**5**), however, showed even greater potency (mean panel GI_{50} approximately 50 nM) and a highly characteristic differential cytotoxicity profile (see Fig. 1). The melanoma panel and some breast, colon, and non-small cell lung cancer lines were quite sensitive to **5**, while the leukemia, renal, and CNS panels were less sensitive.

Several trends were evident from the results of testing this group of compounds. First, the makaluvamine/isobatzelline class (*p*-iminoquinones) is, in general,

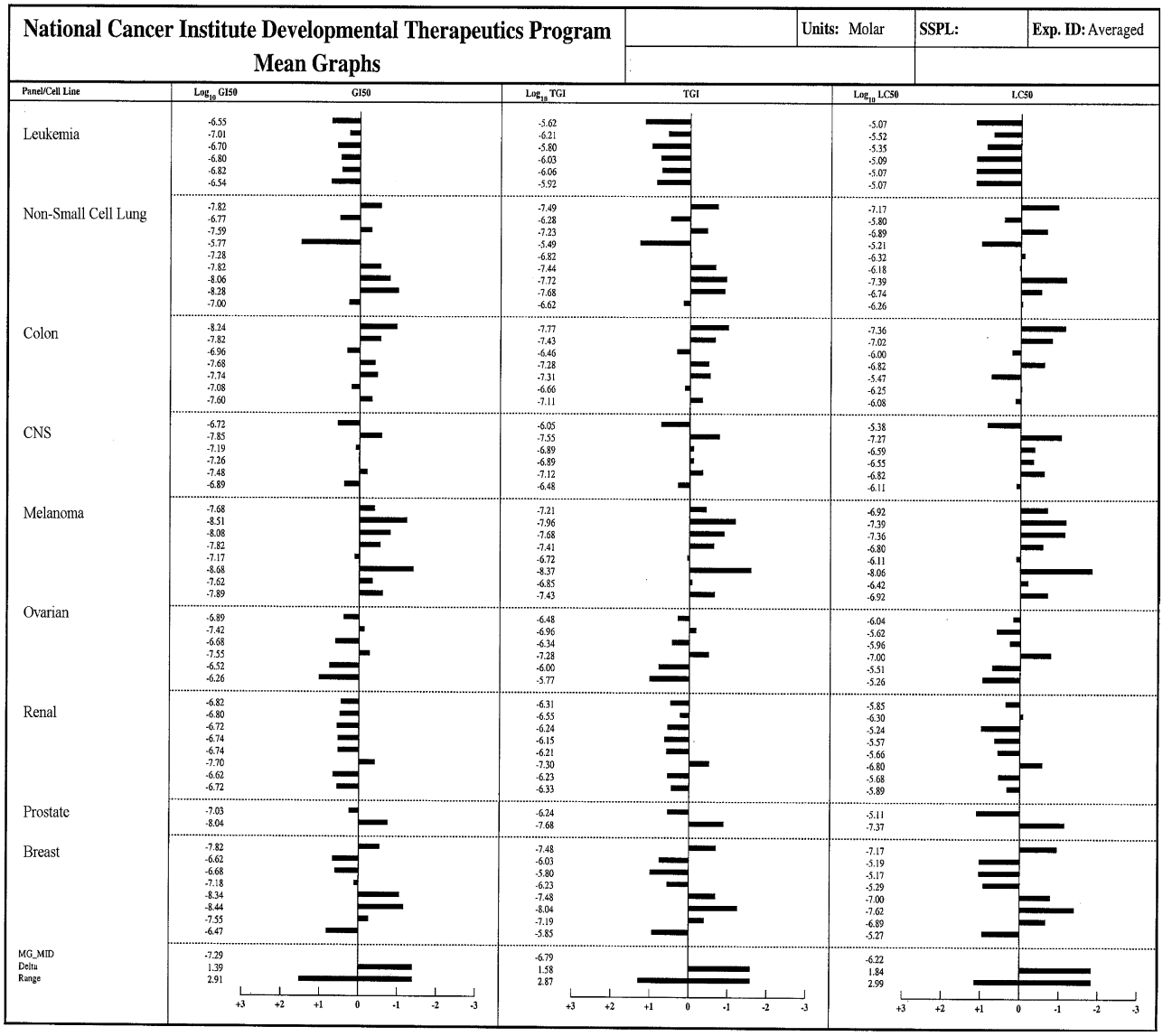

Figure 1. Mean bar graphs for NCI 60 cell line antitumor assay of makaluvamine H (**5**), based on average of quadruplicate tests at three response levels: GI_{50}, TGI, and LC_{50}. Cell lines: leukemia—CCRF-CEM, HL-60(TB), K-562, MOLT-4, RPMI-8226, SR; non-small cell lung—A549/ATCC, EKVX, HOP-62, HOP-92, NCI-H226, NCI-H23, NCI-H322M, NCI-H460, NCI-H522; colon—COLO 205, HCC-2998, NCT-116, NCT-15, NT29, KM12, SW-620; CNS—SF-268, SF-295, SF-359, SNB-19, SNB-75, U251; melanoma—LOX IMVI, MALME-3M, M14, SK-MEL-2, SK-MEL-28, SK-MEL-5, UACC-257, UACC-62; ovarian—IGROV1, OVCAR-3, OVCAR-4, OVCAR-5, OVCAR-8, SK-OV-3; renal—786-0, A498, ACHN, CAKI-1, RXF-393, SN12C, TK-10, UO-31; prostate—PC-3, DU-145; breast—MCF7, MCF7/ADR-RES, MDA-MB-23/ATCC, HS 578T, MDA-MB-435, MDA-N, BT-549, T-47D.

considerably more potent than the batzelline/damirone class (*o*-quinones); the *o*-quinones also exhibit less differential cytotoxicity than the former group (**1** vs **6**; **5** vs **9**). Second, full aromatization of the tricyclic system in **1**–**10** ($\Delta^{3,4}$-series) considerably reduces potency and cell type specificity (**1** vs **2**). Third, a 6-chloro group appears to enhance potency (**1** vs **4**). Fourth, the *N*(5)-methyl substituent also enhances potency (**4** vs **5**).

Since the Ireland/Barrows research collaboration had independently and concurrently identified makaluvamine C (**16**) as the preferred lead compound from this class, makaluvamines C (**16**) and H (**5**) were compared side-by-side against ten cell lines from the NCI panel, revealing that the two compounds were roughly equivalent in potency (Table 3). Makaluvamine H was more potent against five lines, makaluvamine C against two, and the two compounds were equipotent in three. Follow-up quadruplicate testing of **5** and **16** in the full 60 cell line panel provided virtually identical mean GI_{50} values for the two compounds.

2.3. Mechanism of action

In the meantime, efforts to identify the mechanism of action of the makaluvamines were underway. The topoisomerase II-mediated DNA cleavage of various makaluvamines was compared to that of an equimolar concentration of etoposide. Topoisomerase II cleavable complex stabilization could be demonstrated for the

Table 3. Comparative cytotoxicity of makaluvamines C and H

Panel	Cell line	IC_{50} (μg/mL)	
		Makaluvamine C (**16**)	Makaluvamine H (**5**)
Lung	A549	4.13	0.80
	HOP92	2.25	1.05
CNS	SF-295	1.17	0.77
	SF-539	0.68	0.31
	SNB-19	1.20	0.78
Melanoma	LOX	0.54	0.95
	M-14	0.32	0.37
	MALME-3	0.15	0.15
Ovarian	OVCAR-3	0.06	0.25
Breast	MCF-7	0.53	0.50

makaluvamines, but the relative degree of stabilization was markedly less than for etoposide. Makaluvamines H (**5**) and I (**17**) gave the highest percentage of DNA cleavage (33% and 61%, respectively), while the lowest percentages were provided by the *N*(9)-substituted makaluvamines D and V.[27]

Subsequently, we demonstrated that reductive activation of the makaluvamines can also produce DNA damage in vitro. Table 4 shows the percentage of DNA cleavage observed after dithionite reductive activation. Reductive DNA cleavage correlated with two physicochemical parameters of the makaluvamines—the half wave potential ($E_{1/2}$), a measure of the energy necessary to reduce the compound by one electron, and the reversibility parameter ($\delta E_{\text{reduction}}$), a measure of the reversibility of one electron reduction. These data indicated that activation is a two step process initiated by a reversible one electron reduction to generate a radical intermediate. DNA damage could be inhibited by the addition of the radical scavenging agent ascorbate.

The ability of makaluvamines to intercalate with DNA was also measured by fluorescence displacement. Fluorescence displacement curves were generated from the addition of a range of concentrations of pyrroloiminoquinones to genomic salmon testes DNA containing ethidium bromide. From these curves, the values of FC_{50} (concentration reducing fluorescence by 50%) could be calculated. Figure 2 shows the fluorescence displacement curves produced by makaluvamines H and L. The calculated FC_{50} values and standard deviations are summarized in Table 5; these ranged from 1.2 to 40 μM, or 1.2- to 40-fold the amount of ethidium bromide present. The compounds clustered into three distinct groups. Makaluvamines E and L exhibited FC_{50} values of 1.2 and 1.6, respectively, while all but one of the remaining pyrroloiminoquinones had values between 10 and 20; makaluvamine V had the weakest affinity for DNA, with an FC_{50} of 40.

A second, qualitative observation of note concerns the rate of fluorescence attenuation, or steepness of the dose–response curves. The displacement curves for makaluvamines A, C, F, H, I, and N and damirone B appear to change more abruptly from maximal to minimal fluorescence than do the curves representing makaluvamines D, E, L, and V.

While the majority of the makaluvamines were found to have a high affinity for DNA, intercalation efficiency did not correlate with the DNA damage proficiency. This indicates that intercalation is not a limiting step in the generation of DNA damage. However, intercalation may help concentrate the makaluvamines in the nucleus.

Makaluvamines H (**5**) and I (**17**) were chosen for in vivo antitumor evaluation, based on their ability to induce topoisomerase II DNA damage and to damage DNA directly under reductive conditions; makaluvamine H had also exhibited a powerful effect in the NCI 60 cell line tumor panel. In studies published elsewhere,[27] makaluvamines H and I were compared to etoposide in a nude mouse xenograft model using KB tumor cells. The positive control, etoposide, was dosed at 50 mg/kg and gave a T/C 40% (tumor volume in treated mice/tumor volume in untreated control mice). At 22 mg/kg, makaluvamine H gave a response similar to etoposide (T/C 38%), but at less than half the dose (22 vs

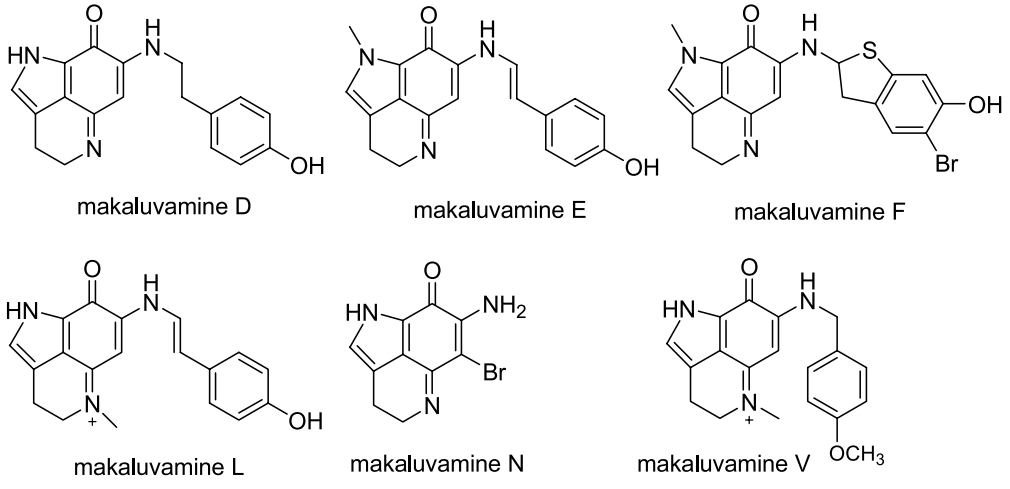

Table 4. Calculated DNA cleavage[a] and one electron reduction parameters

Compound	DNA cleavage/(STD) (%)[b]/(%)[c]	$E_{1/2}$ versus AgCl (V)[d]	$E_{1/2}$ versus NHE (V)[e]	δE_{redn} (V)[f]
Makaluvamine A	50/(4)	−0.453	−0.256	0.061
Makaluvamine C	75/(5)	−0.435	−0.238	0.050
Makaluvamine D	80/(6)	−0.501	−0.304	0.032
Makaluvamine E	63/(3)	−0.420	−0.223	0.053
Makaluvamine F	62/(2)	−0.434	−0.237	0.045
Makaluvamine H	60/(3)	−0.468	−0.271	0.057
Makaluvamine I	85/(4)	−0.406	−0.209	0.044
Makaluvamine L	79/(6)	−0.415	−0.218	0.037
Makaluvamine N	93/(5)	−0.307	−0.173	0.028
Makaluvamine V	73/(4)	−0.460	−0.263	0.054
Doxorubicin	56/(4)	−0.591	−0.394	0.056
Mitoxanthrone	1/(2)	−0.765	−0.568	0.074

[a] Under dithionite reducing conditions.
[b] Mean DNA cleavage ($n = 3$) was calculated by subtracting background amount of nicked DNA present in DNA with STD control reaction from each nicked value after adjusting for total intensity of the DNA in the lane. Amount of nicked DNA remaining is calculated as a percentage of total DNA (supercoiled plus nicked) present in the lane. Higher numbers represent greater DNA cleavage produced by the reduced compounds.
[c] Standard deviations were calculated only to one significant figure, based on the DNA cleavage values from three experiments.
[d] Calculated as the mean of the $E_{forward}$ and $E_{reverse}$ values for each cyclic voltammetry plot.
[e] Standardized electrochemical values referenced to a normal hydrogen electron (NHE), calculated by subtracting 0.197 V from the $E_{1/2}$ values referenced to a Ag/AgCl electrode.
[f] $\delta E_{reduction}$ values are the difference between the $E_{forward}$ and $E_{reverse}$ reactions for one-electron reductions; these are understood to be a measure of reversibility for the reaction.

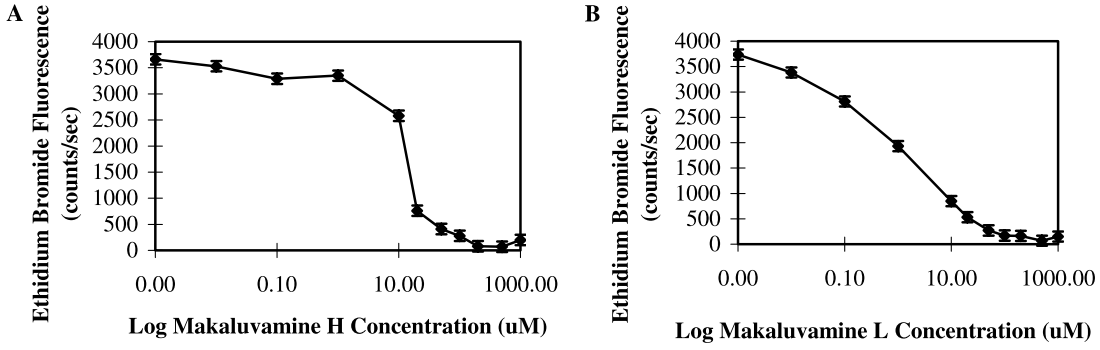

Figure 2. Fluorescence displacement curves for (A) makaluvamine H, and (B) makaluvamine L.

Table 5. Calculated ethidium bromide displacement constants (FC_{50}) for pyrroloiminoquinones

Pyrroloiminoquinone	Mean FC_{50}[a] (μM)	Standard deviation[b] (μM)
Damirone B	18	6
Makaluvamine A	20	5
Makaluvamine C	16	6
Makaluvamine D	10	3
Makaluvamine E	1.6	3
Makaluvamine F	12	2
Makaluvamine H	16	4
Makaluvamine I	17	6
Makaluvamine L	1.2	2
Makaluvamine N	18	5
Makaluvamine V	40	7

[a] Mean FC_{50} values were extrapolated directly from the half-maximal fluorescence values on three displacement curves. Higher numbers represent lesser competition with ethidium bromide, and thus a weaker DNA binding profile.
[b] Standard deviations were calculated to only one significant figure, based on the values of FC_{50} from three curves.

50 mg/kg). Makaluvamine I, at 22 mg/kg, proved toxic (by body weight loss) and the mice received only one injection; nevertheless, a T/C of 34% was achieved.

3. Conclusions

The results presented here and elsewhere[17,26,27] suggest that the cytotoxicity of makaluvamines may be caused by multiple mechanisms or pathways. As a class, the makaluvamines promote topoisomerase II DNA cleavage in vitro; the makaluvamines can also cause direct DNA damage under reductive activation conditions. There may be yet other mechanisms of action involved in the antitumor activity of the pyrroloiminoquinones. In light of these mechanistic insights and demonstrated in vivo and significant differential in vitro activities, makaluvamines H and I may warrant further in vivo evaluation in a broader panel of solid tumors.

4. Experimental

4.1. Collection, extraction, and isolation

Zyzzya sp. was collected at Assail Bank, between North Island and the Wallab Group, Australia (September, 1990). *Z. fuliginosa* was collected on the seaward side of South Murion Island, Australia (August, 1988), off Marchinbar Island, southeast of Cape Wessel, Australia (September, 1990), and in Goss passage near Abrohlos Island, Australia (September, 1990). The latter three collections were originally identified variously as either *Inflatella* sp. or *Z. massalis*, but have all been reclassified as *Z. fuliginosa*, after careful reexamination. The species name *massalis* is now considered invalid and replaced by its senior synonym *fuliginosa*.[28] Voucher specimens are maintained at the Smithsonian Institute Sorting Center, Suitland, MD.

All sponge samples were extracted with the standard National Cancer Institute protocol. Frozen sponge was ground to small pellets in a meat grinder with dry ice and soaked in distilled H_2O at 4 °C for 4 h. The aqueous extract was removed in a basket centrifuge, lyophilized, and weighed. The marc was freeze-dried and then extracted successively with CH_2Cl_2/MeOH (1:1) and MeOH. The combined organic extracts were evaporated in vacuo and weighed (Table 1).

4.1.1. Zyzzya massalis (South Murion Island). A portion of the organic extract (992 mg) was subjected to solvent–solvent partitioning; the aqueous fraction (301 mg) was permeated through Sephadex LH-20 with MeOH/H_2O (9:1) to yield isobatzelline C, **1**, 102 mg (10.3% of the crude extract).

4.1.2. Zyzzya massalis (Marchinbar Island). In one approach, the aqueous extract (1.81 g) was dissolved in 18 mL distilled H_2O; 18 mL EtOH was added and the mixture was stored at −5 °C overnight. The precipitate was separated by centrifugation; the supernatant was evaporated (1.25 g). A portion (224 mg) of the supernatant was permeated through Sephadex LH-20 with MeOH/H_2O (9:1) to yield isobatzelline C, **1**, 44 mg (13.5%). In an alternative approach, the crude aqueous extract (1.177 g) was partitioned between H_2O (100 mL) and *n*-BuOH (3 × 100 mL) to give fractions of 734 and 254 mg, respectively. Some of the aqueous fraction (400 mg) was chromatographed on Sephadex LH-20 as described above to give **1**, 25 mg (3.9%) and **7**, 3 mg (0.5%), while Sephadex LH-20 gel permeation of the *n*-BuOH solubles (184 mg) provided 91 mg of **1** (10.7%) and 29 mg (3.3%) of batzelline C (**6**).

The organic extract (2.9 g) was subjected to solvent–solvent partitioning to give cytotoxic $CHCl_3$ (506 mg) and aqueous MeOH (1.02 g) fractions. The aqueous fraction was essentially pure isobatzelline C (35.2%). The $CHCl_3$ fraction (243 mg) was permeated through Sephadex LH-20 with CH_2Cl_2/MeOH (1:1) to provide a mixture of **1** and **2**. VLC on silica with a $CHCl_3$–MeOH gradient separated the mixture, yielding 25 mg (1.8%) of **1** and 10.5 mg (0.8%) of $\Delta^{3,4}$-isobatzelline C (**2**).

4.1.3. Zyzzya massalis (Goss passage). The aqueous extract (4.43 g) was partitioned between *n*-BuOH and H_2O to give 1.09 g *n*-BuOH solubles and 3.3 g H_2O solubles. Gel permeation of the *n*-BuOH fraction (205 mg) through Sephadex LH-20 with MeOH/H_2O (9:1) gave makaluvamine A, **4**, 10 mg (1.2%). A portion (361 mg) of the aqueous fraction was permeated through Sephadex LH-20 with CH_2Cl_2/MeOH (1:1); a mixture (72 mg) of **4**, **8**, and **12** was obtained. Compounds **8** and **12** were purified by VLC on silica with a $CHCl_3$–MeOH gradient, followed by preparative TLC (silica, $CHCl_3$/MeOH, 7:3); 9.3 mg (1.1%) of **12** and 0.1 mg of **8** were obtained.

4.1.4. Zyzzya sp. (Assail Bank). The organic extract (1.99 g) was partitioned to give cytotoxic $CHCl_3$ (522 mg) and H_2O–MeOH (638 mg) fractions. The latter fraction was mostly makaluvamine H (**5**) by NMR analysis. Purification by Sephadex LH-20 gel permeation gave pure **5** in high yield (16% of the extract). A portion of the $CHCl_3$ fraction (295 mg) was submitted to vacuum liquid chromatography (VLC, silica gel, $CHCl_3$–MeOH gradient) to obtain an additional 53 mg of **5** (4.7%) and fractions containing **9** and **11**. Damirone A (**9**) was purified by reversed phase VLC (C_{18}) with a MeOH–H_2O/HOAc gradient; 17 mg of **9** was obtained (1.5%). The novel compound **11**, 9.4 mg (0.8%), was purified by gel permeation through Sephadex LH-20 with CH_2Cl_2/MeOH (1:1). The remainder (215 mg) of the $CHCl_3$ solubles was chromatographed on Sephadex LH-20 with CH_2Cl_2/MeOH (1:1) to give three cytotoxic fractions. Fraction one gave 14 mg of **9** (1.7%) after successive VLC operations on amino- and C_{18}-bonded phases. Fraction two provided 7.7 mg of **11** (1%) after VLC on silica. Fraction three yielded 2.1 mg of **10** (0.3%) after VLC on C_{18}-bonded phase.

4.1.5. Isobatzelline C (1). Green solid, HRFABMS *m/z* 236.0591 (MH^+, calcd for $C_{11}H_{11}{}^{35}ClN_3O$, 236.0591); ^1H NMR identical to literature report;[11] ^{13}C NMR (Table 2).

4.1.6. Isobatzelline E (2). Orange solid, HRCIMS *m/z* 233.0343 (M^+, calcd for $C_{11}H_8{}^{35}ClN_3O$, 233.0343); UV (MeOH) λ_{max} 224 nm (ε = 21,500), 290 (4800), 422 (13,400); ^1H NMR ($CDCl_3$–CD_3OD, 1:1) δ 4.31 (s, CH_3-1), 6.43 (br s, NH_2-7 in DMSO-d_6), 7.52 (d, J = 6 Hz, H-3), 7.99 (s, H-2), 8.19 (d, 6, H-4);[12] ^{13}C NMR (Table 2).

4.1.7. Makaluvamine A (4). Green solid, DEIMS *m/z* 201 (M^+, $C_{11}H_{12}N_3O$); ^1H NMR (DMSO-d_6), same as reported in literature;[17] ^{13}C NMR (Table 2).

4.1.8. Makaluvamine H (5). Brown-purple solid, HRFABMS *m/z* 216.1129 (MH^+, calcd for $C_{12}H_{14}N_3O$, 216.1137); UV (MeOH) λ_{max} 242 (ε = 1260), 360 (1040), 532 (800); ^1H NMR (CD_3OD) δ 2.98 (t, J = 7.6 Hz, H-3), 3.38 (s, N(5)-CH_3), 3.91 (t, 7.6, H-4), 3.95 (s, CH_3-1), 5.73 (s, H-6), 7.1 (s, H-2); ^{13}C NMR (Table 2).

4.1.9. Batzelline C (6). Brown-purple solid, HRFABMS *m/z* 259.0246 ($[M+Na]^+$, calcd for $C_{11}H_9{}^{35}ClN_2O_2Na$,

259.0251): ^{1}H NMR (CD_3OD) same as reported in literature;[13] ^{13}C NMR (Table 2).

4.1.10. 6-Dechlorobatzelline C (7). Three milligram, HRFABMS *m/z* 203.0821 (MH^+, calcd for $C_{11}H_{11}N_2O_2$, 203.0820); LRFABMS *m/z* 225 ($M+Na^+$, 22%), 203 (MH^+, 15), 176 (38), 154 (100); ^{1}H NMR (DMSO-d_6): δ 8.26 (1H br s), 7.07 (1H, s), 5.01 (1H, s), 3.81 (3H, s), 3.46 (2H, t, $J = 7$ Hz), 2.68 (2H, t, $J = 7$ Hz); ^{13}C NMR (Table 2).

4.1.11. Batzelline D (8). 0.1 mg, HRFABMS *m/z* 223.0279 (MH^+, calcd for $C_{10}H_8{}^{35}ClN_2O_2$, 223.0274); LRFABMS *m/z* 245/247 ($M+Na^+$, 19/6%), 223/225 (MH^+, 28/7), 176 (33), 154 (100), 136 (70); ^{1}H NMR (DMSO-d_6): δ 8.30 (1H, br s), 7.13 (1H, s), 3.58 (2H, t, $J = 7$ Hz) 2.75 (2H, t, $J = 7$ Hz); ^{13}C NMR (Table 2).[12]

4.1.12. Damirone A (9). Brown-purple solid, HRFABMS *m/z* 217.0979 (MH^+, calcd for $C_{12}H_{13}N_2O_2$, 217.0977); ^{1}H NMR (CD_3OD), same as reported in literature;[22] ^{13}C NMR (Table 2).

4.1.13. Damirone B (10). Brown-purple solid, HRFABMS *m/z* 203.0823 (MH^+, calcd for $C_{11}H_{11}N_2O_2$, 203.0821); ^{1}H NMR (CD_3OD), same as reported in literature;[22] ^{13}C NMR (Table 2).

4.1.14. 3,7-Dimethylguanine (12). Colorless solid, HRFABMS *m/z* 180.0892 (M^+, calcd for $C_7H_{10}N_5O$, 180.0885); UV (MeOH) λ_{max} 216 nm ($\varepsilon = 16{,}000$), 238 (7700), 266 (9100); ^{1}H NMR (CD_3OD): δ 3.62 (s, CH_3-3), 3.97 (s, CH_3-7), 6.87 (br s, NH_2, in DMSO-d_6), 7.79 (s, H-8); ^{13}C NMR (CD_3OD): δ 164.9 (C-6), 156.0 (C-2), 150.0 (C-4), 142.6 (C-8), 112.4 (C-5), 33.8 (C-11), 31.4 (C-10).

4.2. Cleavage of DNA produced by dithionite-reduced pyrroloiminoquinones

The reductive cleavage assay was used to compare the pyrroloiminoquinones based on their ability to cause in vitro DNA cleavage under reducing conditions. The reducing agent sodium dithionite (SDT) was used in an adaptation of a protocol published by Islam et al.[29] and Radisky et al.[17]

The optimal conditions, time, and concentrations of the reagents were previously determined by experiments in which the time of incubation and ratios of reagents were varied. This experiment began by adding 4 μL of 1 mM makaluvamines A, C, D, E, F, H, I, L, N, V, or damirone B or control compounds (mitoxantrone and doxorubicin) in DMSO to a 0.75 mL polypropylene microcentrifuge tube. Since DMSO may act as a scavenger of free electrons, the compound-containing tubes were dried in vacuo for 24 h to remove the solvent. From this point on, all manipulations were carried out under argon.

After removal of the solvent, 17 μL of degassed, argon-purged Dulbecco's phosphate buffered saline (PBS) was added to each tube. The tubes were sonicated briefly to aid in the dissolution of the pyrroloiminoquinone. A measure of 1 μL of 1 mg/mL pBR322 supercoiled plasmid DNA was added to each reaction, vortexed, and allowed to equilibrate for 30 min.

A measure of 2 μL of 2 mM SDT in degassed, argon-purged, distilled H_2O was added to each of the reaction tubes to initiate the reactions. Two tubes served as controls, one containing only pBR322 and the other pBR322 plus reducing agent. Final concentrations of all reagents were: 200 μM pyrroloiminoquinone, 200 μM SDT, and 50 ng pBR322 (3.75 μM nucleotide pairs) in a total volume of 20 μL. The reactions were allowed to incubate for 3 h in the dark to allow for reduction of the compounds. The reactions were completed by the introduction of O_2 (air) by vortexing the tubes for 30 min with the caps perforated; the reductive cleavage of DNA occurred after the addition of O_2. The DNA was then precipitated by the addition of 20 μL of 3 M NaOAc, pH 5.5, and 200 μL of EtOH at 0 °C. The solutions were vortexed for 30 s and immersed in crushed dry ice for 1 h. Precipitated DNA was then pelleted by centrifugation at 7000*g* at 4 °C. The supernatant was decanted and the pellet resuspended in 20 μL PBS. To this was added 10 μL loading dye (1% bromophenol blue/50% glycerol/50% of 1× TAE, pH 7.6, w/v/v). The solution was again vortexed and 10 μL was added to a 0.8% agarose, 1× TAE, pH 7.6, gel containing 2 μg ethidium bromide per 100 mL. Electrophoresis was performed for 5 h at 80 V constant voltage in a 1× TAE electrophoresis chamber containing ethidium bromide.

The gel was visualized on a UV transilluminator and photographed. The photographs were then subjected to scanning densitometry to quantify the DNA present in the supercoiled and nicked bands on the gel. The values obtained were listed as a percentage of nicked relative to total DNA. Total DNA was defined as the amount of supercoiled plus nicked in the densitogram. Background nicked DNA visualized in the SDT plus DNA control was subtracted from these values beforehand.

4.3. Ascorbate inhibition of DNA reductive cleavage

To examine whether reductive activation of a pyrroloiminoquinone leads to the potential for radical-mediated damage to DNA, an experiment was conducted using the radical scavenger ascorbate as a trap during the SDT reductive cleavage assay. The experiment was conducted in a manner similar to the previous SDT reductive cleavage assays.

To four 0.75 mL polypropylene microcentrifuge tubes, were added 4 μL of 1 mM makaluvamines C or E in DMSO, two tubes per drug. The tubes were dried in vacuo for 24 h to remove the solvent. All subsequent manipulations were carried out under argon. After drying, 15 μL of degassed, argon-purged PBS, and 1 μL (1 mg/mL) pBR322 supercoiled plasmid DNA were added to each tube. After vortexing and a 30 min equilibration, 2 μL of 100 mM ascorbate, buffered to pH 7.6 with NaOH, was added to each tube, except for the control,

to which 2 μL of distilled H_2O was added. After vortexing, 2 μL of 2 mM SDT in degassed, argon-purged, distilled H_2O was added to each of the reaction tubes to initiate the reactions. Two additional tubes were reserved as controls, one containing only pBR322 DNA and the other containing pBR322 plus dithionite reducing agent. Final concentrations of all reagents were: 200 μM PIQ, 200 μM SDT, 10 mM ascorbate, and 50 ng pBR322 in a total volume of 20 μL. The reactions were allowed to incubate for 3 h in the dark with mixing to ensure complete reduction of the pyrroloiminoquinone in solution. The reactions were completed by the introduction of air, and the DNA was then precipitated by the addition of 20 μL of 3 M NaOAc, pH 5.5, and 200 μL EtOH at 0 °C. The solutions were vortexed for 30 s and immersed in dry ice for 1 h. The samples were then worked up and analyzed by electrophoresis as described above.

The gel was visualized on a UV transilluminator and photographed. The photographs were then subjected to scanning densitometry to quantitate the amount of DNA in the supercoiled and nicked bands on the gel. The amounts were listed as a percentage of the total DNA that was nicked. Total DNA was defined as the amount of supercoiled plus nicked in the densitogram; background nicked DNA visualized in the SDT plus DNA control was subtracted from these values beforehand.

4.4. Determination of pyrroloiminoquinone reductive potentials by cyclic voltammetry

Electrochemistry was performed using a platinum 1.6 mm microdisk working electrode with Ag/AgCl reference and 0.75 mm diameter platinum wire auxiliary electrode. The current was controlled via an RDE-4 Biopotentiostat and the output voltage was monitored by a voltammeter, using the LabView software package (National Instruments, Austin, TX). Background subtraction and analysis made use of Delta Graph 4.0 (Delta Point, Monterey, CA). The scanning rate was 50 mV/s and voltage was scanned from 0 to −800 mV vs the Ag/AgCl reference.

The makaluvamines and controls were prepared by dissolution in 500 μL DMSO, followed by dilution with 4.5 mL PBS, pH 7.4, as the aqueous electrolyte. A background cyclic voltammetry curve of 10% DMSO in PBS, pH 7.4 (v/v) was used for subtraction. Each cyclic voltammetry curve was allowed to reach equilibrium for 10 passes before data collection; all measurements were performed on thoroughly degassed solutions at 23 °C. The results obtained for the reductive cleavage assay and the calculated values of $E_{1/2}$ obtained from the cyclic voltammetry curves were plotted against one another and subjected to linear regression analysis.

4.5. DNA intercalation by the pyrroloiminoquinones

Genomic salmon testes DNA was added to a black 96-well plate at a final concentration of 2 μM nucleotide pairs and 1 μM ethidium bromide in PBS (final concentrations). These concentrations allowed for the maximum number of ethidium bromide binding sites to be filled according to the nearest neighbor exclusion principle.[30] This mixture was allowed to equilibrate for 30 min at 23 °C. After the preincubation period, the pyrroloiminoquinones were added in separate wells across the rows in increasing concentrations (0, 0.01, 0.10, 1.0, 20, 50, 100, 200, 500, and 1000 μM). The first row was reserved for 2 μM DNA plus 1 μM ethidium bromide controls (wells A1–A6) and the fluorescent background of 1 μM ethidium bromide only (wells A7–A12). After a second equilibration for 30 min at 23 °C, the microtiter plates were loaded into the Cytofluor 2300 fluorescent microplate reader. Fluorescent analysis of the wells included excitation via a 530 nm filter (25 nm bandwidth) and a measurement of the concomitant emission using a 620 nm filter (40 nm bandwidth).

The emission measurements were transferred to a Microsoft Excel spreadsheet in which the average background fluorescence of ethidium bromide free in solution (wells A7–A12) was subtracted. The experiment was repeated three times ($n = 3$).

Acknowledgments

We thank P. Murphy (Australian Institute of Marine Science), K. Snader, and D. J. Newman (Natural Products Branch, NCI) for collections, J. Hooper for preliminary taxonomic identifications, T. McCloud for extractions, L. Pannell and G. Gray for the mass spectra, A. Monks and D. Scudiero for the antitumor screens, B. Bath and H. White for assistance with the cyclic voltammetry experiments, M. H. G. Munro for helpful discussions, and M. K. Harper for valuable editorial comments.

References and notes

1. Perry, N. B.; Blunt, J. W.; McCombs, J. D.; Munro, M. H. G. *J. Org. Chem.* **1986**, *51*, 5476–5478.
2. Copp, B. R.; Ireland, C. M.; Barrows, L. R. *J. Org. Chem.* **1991**, *56*, 4596–4597.
3. Molinski, T. F. *Chem. Rev.* **1993**, *93*, 1825–1838.
4. Faulkner, D. J. *Nat. Prod. Rep.* **2002**, *19*, 1–48, and previous reviews in the series.
5. Blunt, J. W.; Copp, B. R.; Munro, M. H. G.; Northcote, P. T.; Prinsep, M. R. *Nat. Prod. Rep.* **2003**, *20*, 1–48.
6. Antunes, E. M.; Copp, B. R.; Davies-Coleman, M. T.; Samaal, T. *Nat. Prod. Rep.* **2005**, *22*, 62–72.
7. Ding, Q.; Chichak, K.; Lown, J. W. *Curr. Med. Chem.* **1999**, *6*, 1–27.
8. Hajdu, E.; van Soest, R. W. M.; Hooper, J. N. A. In *Sponges in Time and Space, Proceedings, 4th International Porifera Congress*; van Soest, R. W. M., Van Kempen, T. M. G., Braekman, J. C., Eds.; Amsterdam, Balkema: Rotterdam, 1993, pp 123–150.
9. van Soest, R. W. M.; Zea, S.; Kielman, M. *Bijdragen tot de Dierkunde* **1994**, *64*, 163–192.
10. (a) Boyd, M. R. In Devita, V. T., Jr., Hellman, S., Rosenberg, S. A., Eds.; Cancer: Principles and Practice of Oncology Updates; Lippincott: Philadelphia, 1989; Vol. 3, pp 1–12; (b) Boyd, M. R. In *Drug Development: Preclinical Screening, Clinical Trials and Approval*; Teicher, B., Ed.; Humana Press: Totowa, NJ, 1997, pp 23–42.

11. Sun, H. H.; Sakemi, S.; Burres, N.; McCarthy, P. *J. Org. Chem.* **1990**, *55*, 4964–4966.
12. Chang, L. C.; Otero-Quintero, S.; Hooper, J. N. A.; Bewley, C. A. *J. Nat. Prod.* **2002**, *65*, 776–778.
13. Sakemi, S.; Sun, H. H. *Tetrahedron Lett.* **1989**, *30*, 2517–2520.
14. (a) Pelletier, S. W.; Chokshi, H. P.; Desai, H. K. *J. Nat. Prod.* **1986**, *49*, 892–900; (b) Coll, J. C.; Bowden, B. F. *J. Nat. Prod.* **1986**, *49*, 934–936.
15. Beutler, J. A.; McKee, T. C.; Fuller, R. W.; Tischler, M., II; Cardellina, J. H., II; McCloud, T. G.; Snader, K. M.; Boyd, M. R. *Antiviral Chem. Chemother.* **1993**, *3*, 167–172.
16. Ireland, C. M.; Radisky, D. C.; Barrows, L. R.; Kramer, R. *US Patent 5,414,001*, issued 9 May 1995.
17. Radisky, D. C.; Radisky, E. S.; Barrows, L. R.; Copp, B. R.; Kramer, R. A.; Ireland, C. M. *J. Am. Chem. Soc.* **1993**, *115*, 1632–1638.
18. Perry, N. B.; McCombs, J.; Copp, B.; Rea, J.; Lill, R.; Major, D.; Andrew, C.; Fulton, K.; Linton, M.; Bringans, S.; Blunt, J. W.; Munro, M. H. G. *Abstract, 37th Annual Meeting*; American Society of Pharmacognosy: Santa Cruz, 1996.
19. Perry, N. B.; Blunt, J. W.; Munro, M. H. G. *J. Nat. Prod.* **1987**, *50*, 307–308.
20. Yagi, H.; Matsunaga, S.; Fusetani, N. *J. Nat. Prod.* **1994**, *57*, 837–838.
21. Cafieri, F.; Fattorusso, E.; Mangoni, A.; Taglialatela-Scafati, O. *Tetrahedron Lett.* **1995**, *36*, 7893–7896.
22. Schmidt, E. W.; Harper, M. K.; Faulkner, D. J. *J. Nat. Prod.* **1995**, *58*, 1861–1867.
23. Stierle, D. B.; Faulkner, D. J. *J. Nat. Prod.* **1991**, *54*, 1131–1133.
24. Dijoux, M.-G.; Gamble, W. R.; Hallock, Y. F.; Cardellina, J. H., II; van Soest, R.; Boyd, M. R. *J. Nat. Prod.* **1999**, *62*, 636–637.
25. Boyd, M. R.; Paull, K. D. *Drug Dev. Res.* **1995**, *34*, 91–109.
26. Barrows, L. R.; Radisky, D. C.; Copp, B. R.; Swaffar, D. S.; Kramer, R. A.; Waters, R. L.; Ireland, C. M. *Anti-Cancer Drug Des.* **1993**, *8*, 333–347.
27. Matsumoto, S. S.; Haughey, H. M.; Schmehl, D. M.; Venables, D. A.; Ireland, C. M.; Holden, J. A.; Barrows, L. R. *Anti-Cancer Drugs* **1999**, *10*, 39–45.
28. Hooper, J. N. A. In *Systema Porifera, A Guide to the Classification of Sponges*; Hooper, J. N. A., van Soest, R. W. M., Eds.; Kluwer Academic Publishers: New York, 2002, pp 412–431.
29. Islam, I.; Skibo, E. B.; Dorr, R. T.; Alberts, D. S. *J. Med. Chem.* **1991**, *34*, 2954–2961.
30. McGhee, J. D.; von Hippel, P. H. *J. Mol. Biol.* **1974**, *86*, 469–489.